Translational Oncology
www.transonc.com

Volume 6 Number 2 April 2013 pp. 169–179 169

Radiosensitization of Glioblastoma Cell Lines by the Dual PI3K and mTOR Inhibitor NVP-BEZ235 Depends on Drug-Irradiation Schedule[1,2]

Sebastian Kuger*, Dorothea Graus*, Rico Brendtke*, Nadine Günther*, Astrid Katzer*, Paul Lutyj*, Bülent Polat*, Manik Chatterjee†, Vladimir L. Sukhorukov‡, Michael Flentje* and Cholpon S. Djuzenova*

*Department of Radiation Oncology, University of Würzburg, Würzburg, Germany; †Department of Internal Medicine II, University of Würzburg, Würzburg, Germany; ‡Department of Biotechnology and Biophysics, University of Würzburg, Würzburg, Germany

Abstract

Previous studies have shown that the dual phosphatidylinositide 3-kinase/mammalian target of rapamycin (PI3K/mTOR) inhibitor NVP-BEZ235 radiosensitizes tumor cells if added shortly before ionizing radiation (IR) and kept in culture medium thereafter. The present study explores the impact of inhibitor and IR schedule on the radiosensitizing ability of NVP-BEZ235 in four human glioblastoma cell lines. Two different drug-IR treatment schedules were compared. In schedule I, cells were treated with NVP-BEZ235 for 24 hours before IR and the drug was removed before IR. In schedule II, the cells were exposed to NVP-BEZ235 1 hour before, during, and up to 48 hours after IR. The cellular response was analyzed by colony counts, expression of marker proteins of the PI3K/AKT/mTOR pathway, cell cycle, and DNA damage. We found that under schedule I, NVP-BEZ235 did not radiosensitize cells, which were mostly arrested in G_1 phase during IR exposure. In addition, the drug-pretreated and irradiated cells exhibited less DNA damage but increased expressions of phospho-AKT and phospho-mTOR, compared to controls. In contrast, NVP-BEZ235 strongly enhanced the radiosensitivity of cells treated according to schedule II. Possible reasons of radiosensitization by NVP-BEZ235 under schedule II might be the protracted DNA repair, prolonged G_2/M arrest, and, to some extent, apoptosis. In addition, the PI3K pathway was downregulated by the NVP-BEZ235 at the time of irradiation under schedule II, as contrasted with its activation in schedule I. We found that, depending on the drug-IR schedule, the NVP-BEZ235 can act either as a strong radiosensitizer or as a cytostatic agent in glioblastoma cells.

Translational Oncology (2013) 6, 169–179

Introduction

Glioblastoma multiforme is the most aggressive primary brain tumor in adults. Standard therapy includes surgical resection followed by radiotherapy, which significantly prolongs survival [1]. Chemotherapy added to radiotherapy is used as concurrent or adjuvant treatment. Although more long-term survivors have been reported after combined chemoradiotherapy [2–4], its success is limited in patients who develop chemoresistance. The induction of chemoresistance is commonly associated with the activation of cell survival pathways and/or aberrations in tumor suppressor genes (for reviews, see [5,6]). Among various survival pathways, the phosphatidylinositide 3-kinase (PI3K)/AKT/mammalian target of rapamycin (mTOR) pathway (hereafter denoted as the PI3K pathway) plays a crucial role in oncogenesis and tumor cell-growth [7]. Its activation can contribute to resistance(s) to chemotherapy and/or radiotherapy by promoting cell survival through prevention of apoptosis [8–11]. Therefore, inhibition of the key proteins in this pathway, such as PI3K, AKT, and/or mTOR, can lead to sensitization of various tumor cell lines to ionizing radiation (IR) [12–17]. A number

Address all correspondence to: Dr Cholpon S. Djuzenova, Department of Radiation Oncology, University of Würzburg, Josef-Schneider-Strasse 11, D-97080 Würzburg, Germany. E-mail: djuzenova_t@klinik.uni-wuerzburg.de

[1]M.C. was supported by the Deutsche Forschungsgemeinschaft (CRU216). Potential conflicts do not exist.

[2]This article refers to supplementary materials, which are designated by Figures W1 to W6 and Tables W1 to W4 and are available online at www.transonc.com.

Received 22 October 2012; Revised 10 January 2013; Accepted 11 January 2013

DOI 10.1593/tlo.12364

of pharmacological inhibitors of the PI3K pathway are known to synergistically enhance the cytotoxicity of IR [13–15,17,18]. Examples of the single-target inhibitors of the first generation are LY294002 [18] and wortmannin [14] (both inhibitors of PI3K), as well as the mTOR inhibitor rapamycin [17], which have been shown to enhance the radiation sensitivity of several tumor cell lines. A major drawback of the single-target inhibitors (either PI3K or mTOR), however, is the induction of a feedback loop resulting in a compensatory stimulation of AKT, which in turn activates pro-survival signaling [19–21]. Moreover, some of the first-generation inhibitors have revealed low specificity, instability, or insolubility (reviewed in [22]) and have also caused severe side effects in mouse model, such as respiratory depression and lethargy [23].

There has been considerable effort to design small synthetic inhibitors of the PI3K pathway with improved selectivity and pharmaceutical properties. Both requirements are met by NVP-BEZ235, an imidazoquinoline derivate, which simultaneously inhibits pan-class I PI3K and mTOR kinases [24]. This novel orally available dual PI3K and mTOR inhibitor has revealed potent antitumor activity in several *in vitro* and *in vivo* studies [25–28]. In addition, the substance enhances the radiation sensitivity of several tumor cell lines *in vitro* [29–33] as well as in tumor model *in vivo* [29,32,33]. According to the studies quoted above [29,30,32,33], NVP-BEZ235 exerts radiosensitizing antitumor effects if it is added to tumor cells shortly before irradiation and cells are kept in drug-containing medium for up to 24 hours after irradiation. In contrast, Fokas et al. have found no radiosensitization of laryngeal SQ20 and bladder T24 tumor cell lines if NVP-BEZ235 was added 6 hours after IR for a total exposure time of 18 hours [21].

To prove whether the time schedule of NVP-BEZ235 and IR administration is critical for radiosensitization, we explore in the present study the response of four established glioblastoma cell lines to two different drug-IR schedules. In schedule I, tumor cells were incubated with the drug for 24 hours, but shortly before IR the substance was washed out. In schedule II, the inhibitor was added to the cells 1 hour before IR and kept in culture medium up to 48 hours after IR. Cells treated according to the different drug-IR schedules were analyzed for colony-forming ability, induction and repair of radiation-induced DNA damage, and cell cycle distribution. In addition, the expression levels of several marker proteins (PTEN, PI3K, AKT, phospho-AKT, mTOR, phospho-mTOR, phospho-4E-BP1, S6, phospho-S6 ribosomal protein, etc.) were assessed by Western blot analysis.

Materials and Methods

Cells

The group of human glioblastoma cell lines examined includes GaMG (PTEN wt, p53 mut), DK-MG (PTEN wt, p53 wt), U373 (PTEN mut, p53 mut), and U87-MG (PTEN mut, p53 wt) cells. All cell lines were obtained from the American Type Culture Collection (Manassas, VA) and routinely cultured under standard conditions (5% CO_2, 37°C) in complete growth medium (CGM), which was either Dulbecco's modified Eagle's medium (GaMG, DK-MG) or minimum essential medium (U373, U87-MG), supplemented with 10% FBS.

Drug Treatment

The dual PI3K and mTOR inhibitor NVP-BEZ235 [24] was kindly provided by Novartis Institutes for Biomedical Research (Basel, Switzerland). The drug was freshly diluted from frozen aliquots in DMSO stored at −20°C. Drug (100 nM) and radiation treatments were applied in two different schedules (Figure 1). In schedule I, the substance was added 24 hours before IR and washed out shortly before irradiation. Under schedule II, the drug was added 1 hour before IR and remained in CGM up to 48 hours after IR. Cells treated in parallel with respective amounts of DMSO served as controls.

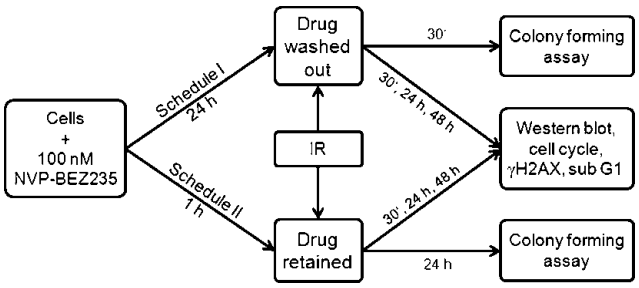

Figure 1. Two different drug-IR schedules were used in this study. Schedule I: NVP-BEZ235 was added to the tumor cell cultures for 24 hours and washed out shortly before IR. Schedule II: NVP-BEZ235 was added to the cell cultures 1 hour before IR and kept in culture medium up to 48 hours after IR. Cells treated in different schedules were then analyzed by colony-forming ability, expression of marker proteins, DNA damage, and cell cycle progression.

Antibodies

The primary and secondary antibodies are specified in Supplementary Materials.

Cell Viability Assay

The intracellular ATP level, as an indicator of cell viability, was determined by means of the CellTiter-Glo Luminiscent Cell Viability Assay (Promega, Madison, WI) according to the manufacturer's instructions. Serial dilutions of NVP-BEZ235 (0–5 μM) in CGM were added to cell cultures in quadruplicates and the cytotoxicity of the drug was determined 24 and 48 hours later. Control samples contained the respective concentrations of DMSO. The mean ATP content data (±SD) from three independent experiments were normalized against DMSO-treated controls to generate dose-response curves and then analyzed with the standard four-parameter logistic model (4PLM, Equation 1):

$$Y = \frac{A_1 - A_2}{1 + (c / \mathrm{IC}_{50})^p} + A_2, \qquad (1)$$

where Y is the cell viability, c is drug concentration given in nM, A_1 and A_2 are the upper and lower asymptotes, respectively, IC_{50} is the 50% inhibitory concentration (nM), and p is the Hill slope.

Colony Survival Assay

Cell survival curves were generated by a standard colony formation assay as previously described [34]. Subconfluent monolayers of drug-treated and non-treated cells were irradiated in culture flasks filled with CGM at room temperature by graded single doses (0–8 Gy), seeded either immediately (schedule I) or 24 hours (schedule II) after IR in Petri dishes and then cultivated in CGM for the next 2 weeks. Four replications were carried out for each exposure point, and the

experiments were repeated at least twice. After 2 weeks, the cells were fixed and stained with crystal violet (0.6%). Colonies of at least 50 cells were scored as survivors. The mean survival data for each individual cell line were fitted to the linear quadratic (LQ) model (Equation 2):

$$SF = \exp\left(-\alpha X - \beta X^2\right), \quad (2)$$

where SF is the survival fraction, X is the irradiation dose, and α and β are the fitted parameters.

Western Blot

For immunoblot analysis, whole-cell lysates were prepared according to standard procedures. Samples equivalent to 20 to 40 μg of protein were separated using 4% to 12% sodium dodecyl sulfate–polyacrylamide pre-cast gels (Invitrogen, Karlsruhe, Germany) and transferred to nitrocellulose membranes. For protein detection, membranes were incubated with respective primary and species-specific peroxidase-labeled secondary antibodies according to standard protocols. The levels of protein expression were quantified using the Kodak 1D Image analyzing software (Scientific Imaging Systems, Eastman Kodak Company, Rochester, NY) and normalized to the β-actin levels.

X-ray Irradiation

Irradiation was performed at room temperature using a 6-MV Siemens linear accelerator (Siemens, Concord, CA) at a dose rate of 2 Gy/min. After irradiation, cells were kept in CGM for the indicated time until harvest.

Detection of Histone γH2AX and Cell Cycle Measurements by Flow Cytometry

Non-treated and drug-treated cell cultures were irradiated as subconfluent monolayers in CGM at room temperature. The cells were then incubated under standard conditions and analyzed by flow cytometry 30 minutes, 24 hours, and 48 hours after IR exposure. For analysis, cells were trypsinized, washed twice in phosphate-buffered saline, fixed, and stained for γH2AX according to a protocol described elsewhere [35]. The cells were then counterstained with propidium iodide (PI, Sigma P-4170, 10 μg/ml) in the presence of RNase A (Sigma R-5250, 25 μg/ml) as described elsewhere [36]. At least 15,000 cells were assayed for either histone γH2AX, DNA distribution, or fraction of cells with hypodiploid DNA content using a flow cytometer FACSCalibur (Becton Dickinson, San Jose, CA) equipped with a 15-mW argon-ion laser. Cellular green (histone γH2AX) or red fluorescence (DNA-PI) was acquired in logarithmic or linear mode, respectively. The output data presented as one-dimensional histograms, i.e., the distributions of histone γH2AX or PI-DNA signals within cell samples, were analyzed using the Flowing Software program obtained from P. Terho (Turku Centre for Biotechnology, Turku, Finland) and the ModFit LT program (Verity Software House, Topsham, ME).

Statistics

Data are presented as means (±SD or ±SE). Mean values were compared by the Student's t test. The threshold of statistical significance was set at $P < .05$. Statistics and fitting of experimental data were performed with Origin 8.5 (Microcal, Northampton, MA).

Results

Effects of NVP-BEZ235 on Cell Proliferation and Colony Survival

The cytotoxic potential of NVP-BEZ235 against *non-irradiated* tumor cells was studied over a concentration range from 10 nM to 1 μM. Cell viability was quantified by an ATP-based assay. The cellular ATP levels in drug-treated samples were normalized against DMSO-treated controls, plotted *versus* the drug concentration (Figure W1), and fitted to the 4PLM (Equation 1). As seen in Figure W1, the ATP content in four tested cell lines depends not only on drug concentration but also on the duration of drug treatment. With increasing NVP-BEZ235 concentration, the mean ATP content in all cell lines decreased steadily to reach a plateau at about 60% to 70% and 40% to 50% of the initial level after a 24-hour and a 48-hour drug exposure, respectively. In all cell lines, the maximum ATP inhibition was achieved at NVP-BEZ235 concentrations ≥100 nM. On the basis of these measurements, a drug concentration of 100 nM was used for subsequent experiments. The selected inhibitor concentration is consistent with the previously reported data [24,37].

Using the colony survival assay, we analyzed in the following experiments the radiation sensitivities of glioblastoma cells treated with NVP-BEZ235 according to two different drug-IR schedules presented schematically in Figure 1. Figure 2 shows the normalized cell survival responses of drug-treated cells plotted *versus* the radiation dose, along with the best fits of the LQ model (Equation 2) to the data. The plating efficiencies (PEs) of non-irradiated cell samples, as well as the fitted parameters derived with the LQ model, including the surviving fraction at 2 Gy (SF2), the radiation dose required to reduce colony forming ability by 90% (D_{10}), and the growth inhibition factor (I_{10}), are summarized in Table W1.

The data shown in Figure 2 and Table W1 prove that NVP-BEZ235 did not affect the radiosensitivity of glioblastoma cells treated according to schedule I. At the same time, NVP-BEZ235 acted as a potent radiosensitizer in all tested cell lines treated with schedule II (Figure 2, bottom row), which is also evident from the markedly reduced SF2 and D_{10} values (Table W1) in drug-treated samples. The radiosensitizing activity of NVP-BEZ235 in glioblastoma cell lines was independent of their PTEN and p53 mutational status.

Changes in the PI3K Pathway Induced by NVP-BEZ235 and/or Radiation

To elucidate the molecular basis for the distinct radiation responses of tumor cells treated with different drug-IR schedules (Figure 2), we analyzed the expression of several marker proteins of the PI3K pathway by Western blot analysis. Figure 3 shows exemplarily the Western blot data of control and drug-treated DK-MG and U87-MG cells probed for PTEN, PI3K (110 and 85 kDa), phospho-AKT, AKT, phospho-mTOR, mTOR, phospho-S6, and phospho-4E-BP1 30 minutes after irradiation with 8 Gy. Samples shown on the left- and right-hand sides of Figure 3 were treated according to schedules I and II, respectively. The data for the other tested cell lines at 30 minutes are shown in Figure W2. The expressions at 24 and 48 hours after IR are shown in Figures W3 and W4, respectively.

As expected, PTEN protein was detected only in DK-MG cells that are wild-type PTEN, whereas the PTEN mutated U87-MG cell line showed no expression of PTEN at all (Figure 3). Furthermore, the background expression levels of phospho-AKT and phospho-mTOR in U87-MG cells were much higher than in DK-MG cells,

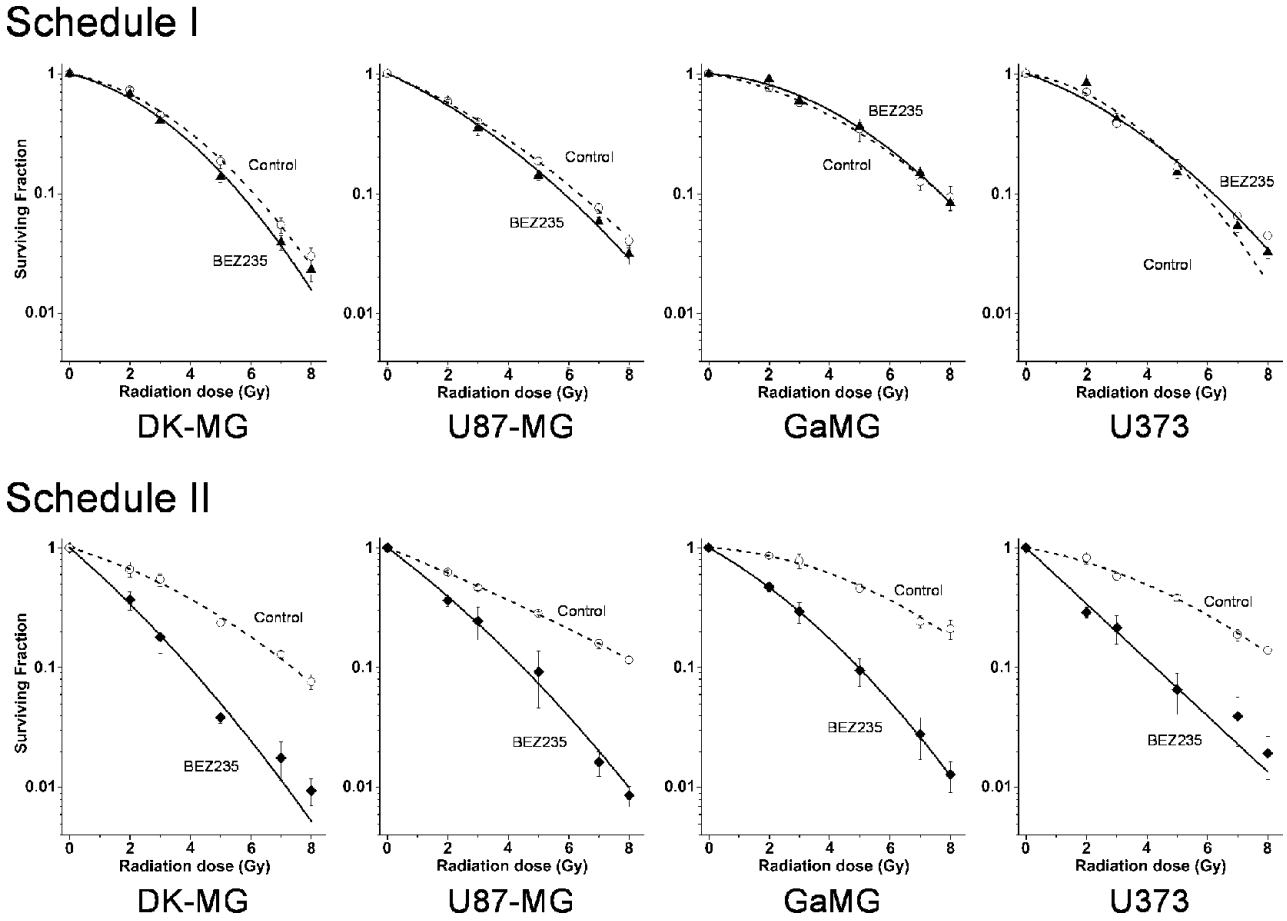

Figure 2. Clonogenic survival of glioblastoma cell lines treated with NVP-BEZ235 and irradiated either in schedule I (top row) or schedule II (bottom row); for details on treatment, see Figure 1. Irradiated cells were plated for the colony-forming test either immediately after IR (top row) or 24 hours after IR (bottom row). After 2 weeks, colonies containing at least 50 cells were scored as survivors. Data derived from at least four independent experiments for each cell line and schedule were pooled together and fitted by an LQ equation (Equation 2). The SD values are indicated by error bars.

which can be associated with the lack of PTEN in U87-MG cells leading to a compensatory activation of the PI3K pathway.

In non-irradiated DK-MG cells treated with schedule I, NVP-BEZ235 caused a moderate increase of p110α subunit of PI3K and also two-fold increases of phospho-AKT (0.26→0.55 a.u.) and phospho-mTOR (0.33→0.67 a.u.; Figure 3*A*). At the same time, treatment of U87-MG cells using schedule I without IR induced almost no changes in the expression of all tested proteins, except for phospho-AKT whose expression slightly increased from 1.06 to 1.24 a.u. In contrast, treatment of cells according to schedule II strongly reduced the expressions of phospho-AKT and phospho-mTOR after a short (1 hour) incubation with NVP-BEZ235 in both cell lines, with or without radiation. Two other tested cell lines, GaMG and U373, showed qualitatively similar data on the expression of marker proteins detected 30 minutes or 24 and 48 hours (Figures W2–W4) after IR.

We also analyzed the expression of ribosomal S6 and translational repressor 4E-BP1 proteins, which are downstreams of mTOR known to influence cell cycle progression and growth regulation [38,39]. Thirty minutes after IR under schedule I (Figures 3 and W2, left panel), phospho-S6 protein was completely suppressed in drug-pretreated cells but mostly recovered to the normal level after washing out NVP-BEZ235 (Figures W3 and W4, *A* and *B*). In contrast, treatment of cells with NVP-BEZ235 according to schedule II altered the expression of phospho-S6 protein immediately (30 minutes) after irradiation to a much lesser extent (Figures 2 and W2, right side) than under schedule I. However, at 24 and 48 hours after IR, this protein was nearly depleted under schedule II (Figures W3 and W4, right side). The expression of phospho-4E-BP1 remained almost unchanged in cells treated according to schedule I throughout the experiment (i.e., 30 minutes to 48 hours after IR). In contrast, the addition of NVP-BEZ235 according to schedule II led to a strong depletion of phospho-4E-BP1 over the whole observation time (30 minutes to 48 hours).

Assessment of Late-Stage Apoptosis

Further efforts to identify the mechanism(s) of radiosensitizing effects of NVP-BEZ235 on glioblastoma cells seen under schedule II were made by measuring late-stage apoptosis using flow cytometry. Figure 4 shows exemplarily the DNA content distributions in GaMG cells treated with NVP-BEZ235 and IR according to schedules I and II analyzed by flow cytometry 24 and 48 hours after irradiation with 8 Gy. From the DNA histograms, the fractions of hypodiploid cells were evaluated to assess the extent of late-stage apoptosis. As seen in Figure 4 (right hand side, bottom row), combined drug-IR treatment according to schedule II significantly increased the portion of

hypodiploid GaMG cells up to 54%, compared to the 9.6% detected in control irradiated cells. Qualitatively similar results were obtained with DK-MG and U373 cells but not with U87-MG cells (Figure W5). The increased fraction of hypodiploid cells and debris in GaMG, DK-MG, and U373 cells was found to correlate with the increased level of cleaved poly (ADP-ribose) polymerase (PARP) an established pro-apoptotic marker, in these cell lines (Figures W2–W4). Unlike schedule II, drug-IR treatment according to schedule I did not induce apoptosis in GaMG cells, as suggested by the nearly unchanged fraction of hypodiploid cells (~10%; Figure 4, third row) with respect to drug-free control (~8%).

Induction and Decay of Histone γH2AX

The degree of DNA damage induced in glioblastoma cell lines by two different drug-IR treatment schedules was assessed by immunostaining and flow cytometric detection of histone γH2AX, a sensitive marker of DNA double-strand breaks [40]. The expression of histone γH2AX was determined 30 minutes, 24 hours, and 48 hours after irradiation (Figures 5*A* and W6, *A*–*C*).

As evident from Figures 5*A* and W6, *A* to *C* (top rows), the radiation-induced DNA damage in glioblastoma cells was only little, if at all, affected by NVP-BEZ235 when cells were treated according to schedule I. Moreover, 30 minutes after IR under schedule I, the drug-IR treated GaMG cells exhibited even less DNA damage (69 a.u. of γH2AX; Figure 5*A*) than the corresponding irradiated drug-free controls (101 a.u.). As with the initial IR-induced DNA damage, NVP-BEZ235, given under schedule I, did not noticeably affect the DNA damage repair process in glioblastoma cell lines, as suggested by the rapid reduction of γH2AX observed 24 and 48 hours after IR (middle and bottom rows in Figure 5*A*).

Under schedule II, NVP-BEZ235 increased nearly four-fold the initial IR-induced DNA damage in GaMG cells (43→169 a.u. of γH2AX), compared to a 3.4-fold increase in drug-free control (66→226 a.u.). Among the four cell lines, a drug-mediated induction of DNA damage under schedule II also occurred in DK-MG and U373 cells (Figure W6, *A* and *C*) but was less evident in U87-MG cells (Figure W6*B*). Despite lower or similar initial damage, the DNA damage repair was severely impaired in all glioblastoma cell lines treated with NVP-BEZ235 according to schedule II, compared to drug-free controls and also to schedule I.

Prompted by the observation that drug-IR treatment under schedule II increased DNA damage and impaired its repair, we analyzed the expression of the DNA repair protein Rad51. Recently, the expression of this protein has been found to be abrogated by NVP-BEZ235 [32]. Figure 5*B* shows representative Western blot detections of Rad51 protein in DK-MG and U87-MG cell lines treated with two different drug-IR schedules. In agreement with [32], we found that NVP-BEZ235 strongly inhibited the expression of Rad51 protein (Figure 5*B*). Thus, with increasing incubation time with NVP-BEZ235 from 30 minutes to 48 hours under schedule II, the Rad51 contents decreased steadily from 0.73 to 0.13 a.u. in non-irradiated DK-MG cells and from 1.05 to 0.33 a.u. in non-irradiated U87 cells. Combined drug-IR treatment caused further depletion of Rad51 in U87 cells (but not in DK-MG).

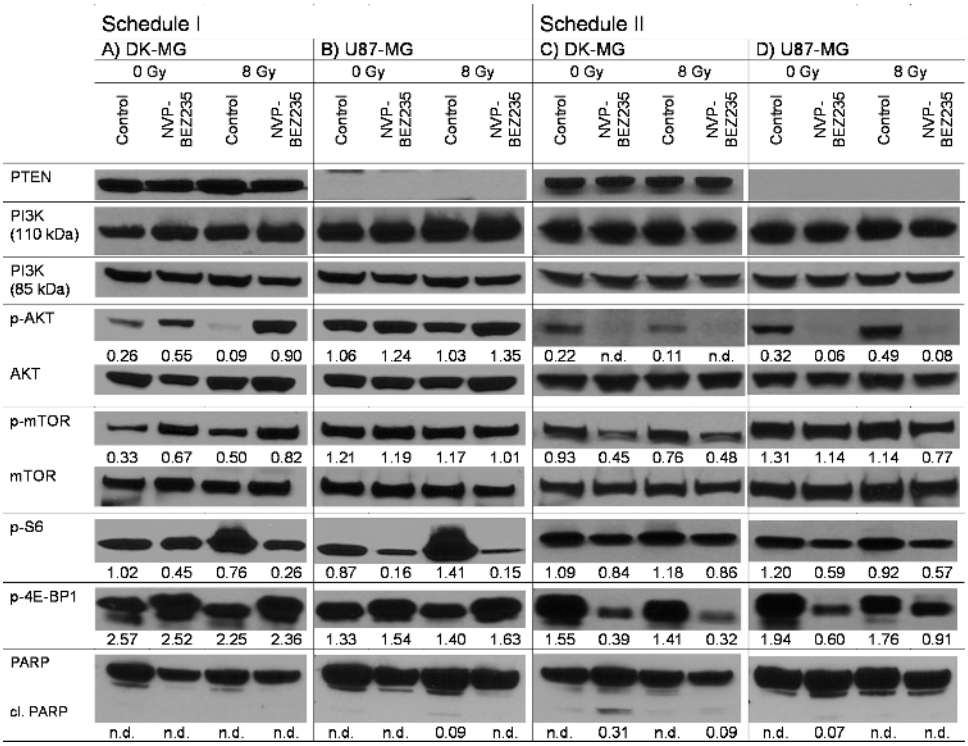

Figure 3. Representative Western blot analysis of expression levels of several marker proteins of the PI3K pathway. DK-MG (A, C) and U87-MG (B, D) tumor cell lines were subjected to drug and IR treatments according schedule I (A, B) or schedule II (C, D). Cellular lysates were prepared 30 minutes after irradiation with 8 Gy. Each protein band was normalized to the intensity of β-actin used as loading control, and the ratios are denoted by the numbers if significant changes in the expression are present. The experiment was repeated at least three times. n.d. indicates not determined.

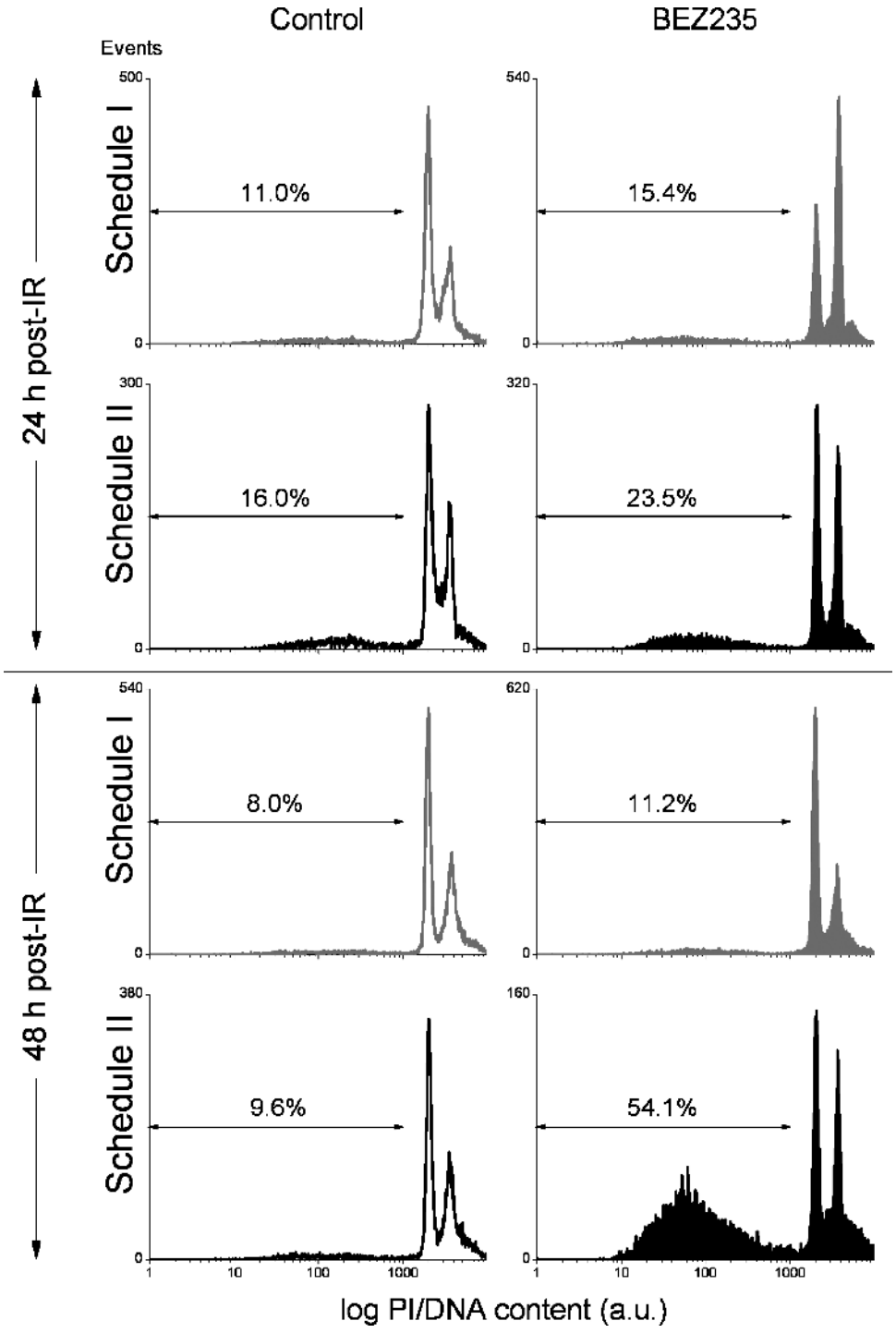

Figure 4. Percentage of cells with hypodiploid DNA content and cellular debris in drug-treated and irradiated GaMG tumor cell line measured flow cytometrically. Cells were subjected to drug-IR treatments according to schedule I (gray histograms) or schedule II (black histograms). Unfilled histograms represent control drug untreated cells. Twenty-four or 48 hours after IR, the cells were detached with trypsin, treated with saponin and RNAse, stained with PI, and then analyzed for red fluorescence by flow cytometry. The samples include both floating and trypsinized cells. Depicted are the percentages of events for hypodiploid nuclei and debris, computed by means of the Flowing Software. The results are representative of three independent experiments.

Cells treated with schedule I (i.e., a 24-hour preincubation with NVP-BEZ235) also displayed low levels of Rad51 (0.31 a.u. in DK-MG and 0.18 a.u. in U87-MG). However, 24 hours after washing out the inhibitor, the expression of Rad51 returned back to the control levels of 0.73 and 0.81 a.u. in DK-MG and U87 cells, respectively. Qualitatively similar results were obtained with GaMG and U373 cell lines. The expression of another tested DNA repair protein Rad50 was not affected by NVP-BEZ235 treatment (data not shown).

Effects of NVP-BEZ235 and IR on Cell Cycle Progression

Further efforts to identify the mechanisms underlying the radiosensitizing effect of NVP-BEZ235 used only under schedule II and

not under schedule I were focused on the possible impact of the drug on cell cycle progression. Figure 6 shows representative cell cycle histograms for DK-MG cells, whereas the summarized data for all tested cell lines are shown in Tables W2–W4. The large portions of cells in the S and G_2/M phases (G_2/G_1 ratio of ~0.6) in untreated cells in Figure 6 (top row) prove that the cell culture was in the exponential growth phase at the beginning of the experiments. A 24-hour incubation with NVP-BEZ235 under schedule I caused an enrichment (up to 70%) of G_1 cells, whereas the G_2/G_1 ratio sank to ~0.25. Upon washing out the drug, the cells were released from the G_1 block, and the G_2/G_1 ratio increased to ~0.6 (Figure 6, fourth row, left histogram).

Independent of the treatment schedule, irradiation with 8 Gy resulted in an accumulation of cells in the G_2/M phase of the cell cycle

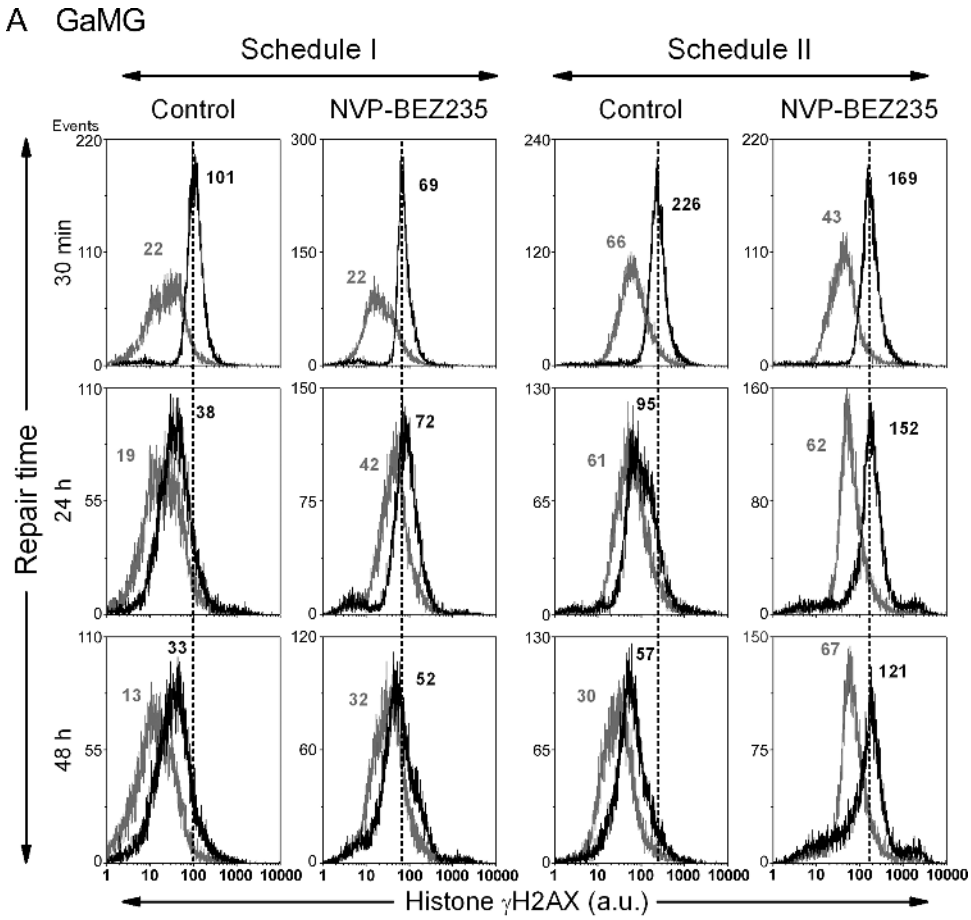

Figure 5. Representative distributions of nuclear histone γH2AX (A) in GaMG glioblastoma cell line, detected 30 minutes, 24 hours, and 48 hours after irradiation with 8 Gy and after a combined drug-IR treatment either according schedule I (two top rows) or schedule II (third and fourth rows) by means of flow cytometry. Black and light gray histograms represent irradiated and non-irradiated cells, respectively. Numbers denote the mean histone γH2AX expression for the respective cell sample. Expression levels of the DNA repair protein Rad51 (B) detected in DK-MG and U87-MG cell lines treated in different drug-IR schedules. The experiment was repeated four times.

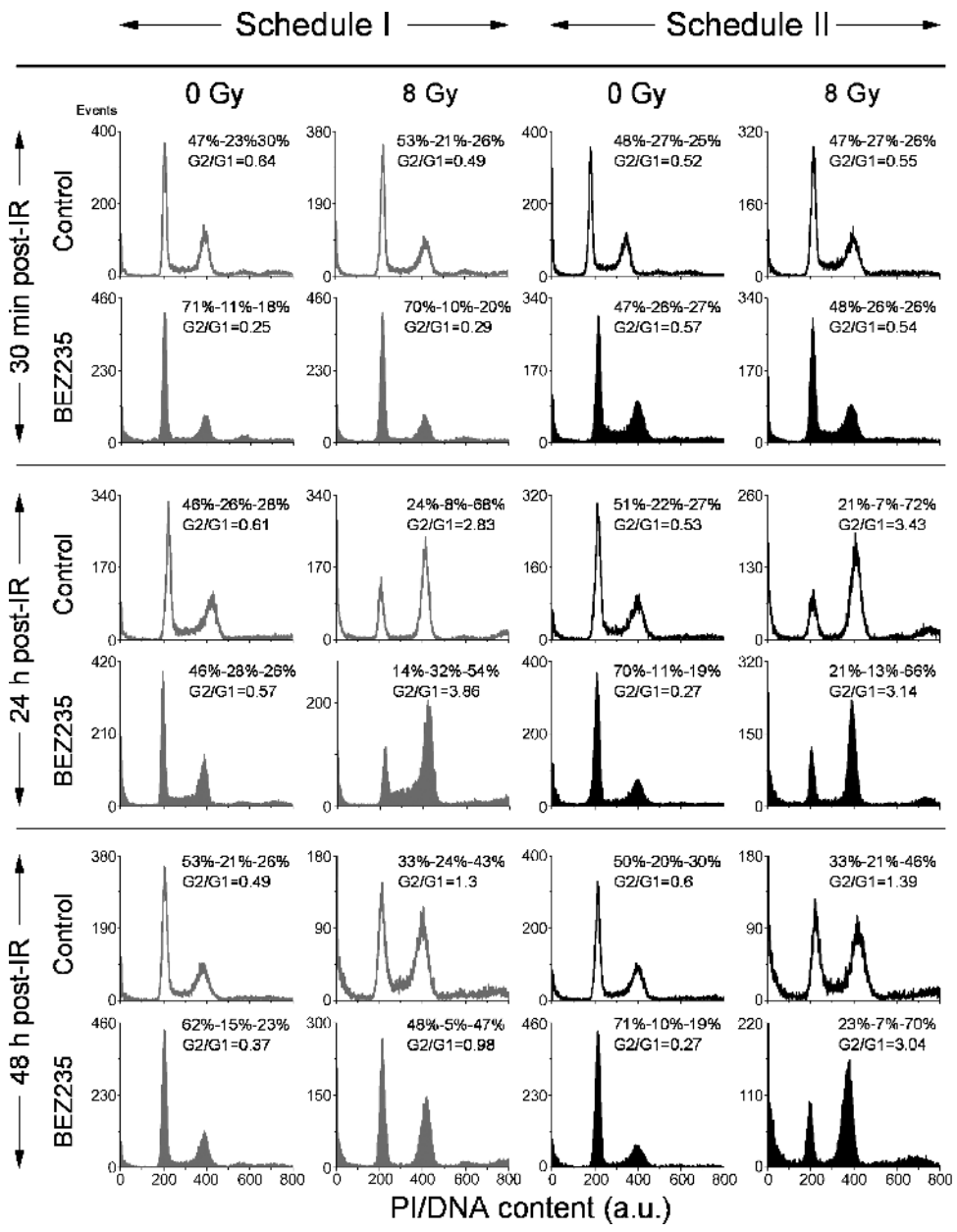

Figure 6. Effects of NVP-BEZ235, ionizing radiation (IR), and combined drug-IR treatment on the cell cycle phase distribution in DK-MG cell line. Cells were subjected to combined drug-IR treatment according schedule I (first and second columns from the left) or schedule II (third and fourth columns). After IR with 8 Gy, cells were cultured for 30 minutes, 24 hours, or 48 hours, fixed, permeabilized, stained with PI, and analyzed for DNA content by flow cytometry using linear signal amplification. DNA histograms were deconvoluted with ModFit Software. Numbers denote the percentage of cells in G_1, S, and G_2/M phases and G_2/G_1 ratios in each cell sample. The data are representative of at least five independent experiments.

24 hours after IR (Figure 6). Combined drug-IR treatment under schedule II showed strong depletion of S phase cells (13%) compared with that in schedule I (32%). Forty-eight hours after IR, combined drug-IR treatment strongly depleted (by a factor of 3–4) the fraction of S phase cells, under both treatment schedules. However, the arrest under schedule I was reversible and the cell cycle normalized 48 hours after IR. In contrast, under schedule II, the G_2/M arrest persisted up to 48 hours after IR.

To sum up, pretreatment with NVP-BEZ235 under schedule I caused a G_1 arrest before IR, which was reversible upon drug withdrawal. Combined NVP-BEZ235 and IR treatment caused a strong G_2/M arrest 24 hours after IR in both schedules; under schedule II, the arrest was prolonged up to 48 hours after IR.

Discussion

Clinicians have combined chemotherapy and radiation therapy since the 1980s [41] and the combination of radiation and concurrent chemotherapy or molecularly targeted therapy has been convincingly shown to be superior to radiation alone in treatment of several cancer forms [42]. Among other factors, the efficacy of the combined radiochemotherapy is dependent on the schedule of drug administration [42]. Particularly, the combination of gemcitabine followed

by gefitinib (an inhibitor of the epidermal growth factor receptor) has been found be more effective in controlling tumor growth than the reverse drug schedule [42].

The present study was designed to prove whether the schedule of NVP-BEZ235 and IR administration is critical for radiosensitization. A major new finding of this study was that, depending on the drug-IR schedule, the dual PI3K/mTOR inhibitor NVP-BEZ235 promoted either radiosensitization or a cytostatic effect in glioblastoma cell lines. The drug acted as a potent radiosensitizer only if added to cells *shortly before IR* and kept in culture up to 24 hours thereafter (schedule II), as evidenced by the colony counts shown in Figure 2 (bottom row). The radiosensitizing effect was independent of the PTEN and p53 status of the cell lines. The enhancement of radiation sensitivity by NVP-BEZ235 under schedule II reported here is consistent with the recent findings that, if added shortly before IR, NVP-BEZ235 radiosensitizes various tumor cell lines [29–33]. At variance with schedule II, a long-term pretreatment of cells with NVP-BEZ235 (schedule I) completely abolished the radiosensitizing ability in all of tested glioblastoma lines (Figure 2, top row).

To elucidate the dependence of the radiosensitizing activity of NVP-BEZ235 on the drug-IR schedule, we thoroughly examined the expression of several key proteins of the PI3K pathway, the degree of late-stage apoptosis, induction and repair of DNA damage, and cell cycle distribution. The observed differences between cellular responses to combined drug-IR treatment used under two different schedules can be explained by a simplified model illustrated in Figure 7. The model takes account of the different expression of marker proteins of the PI3K/mTOR pathway (Figures 3 and W2–W4), which was dependent on the incubation time with the drug. The model also includes additional data on the colony counts, DNA damage, and cell cycle-progression given in Figures 2, 5, 6, and W2 to W6 and Tables W1 to W4.

Surprisingly, our Western blot analysis revealed that the long-term pretreatment with NVP-BEZ235 according to schedule I caused an *up-regulation* of the phosphorylated forms of AKT and mTOR (Figure 7*A*) in three of four cell lines studied here (Figures 3 and W2). The effect was even stronger after combined drug-IR treatment. The increased expression of phospho-AKT and phospho-mTOR suggests

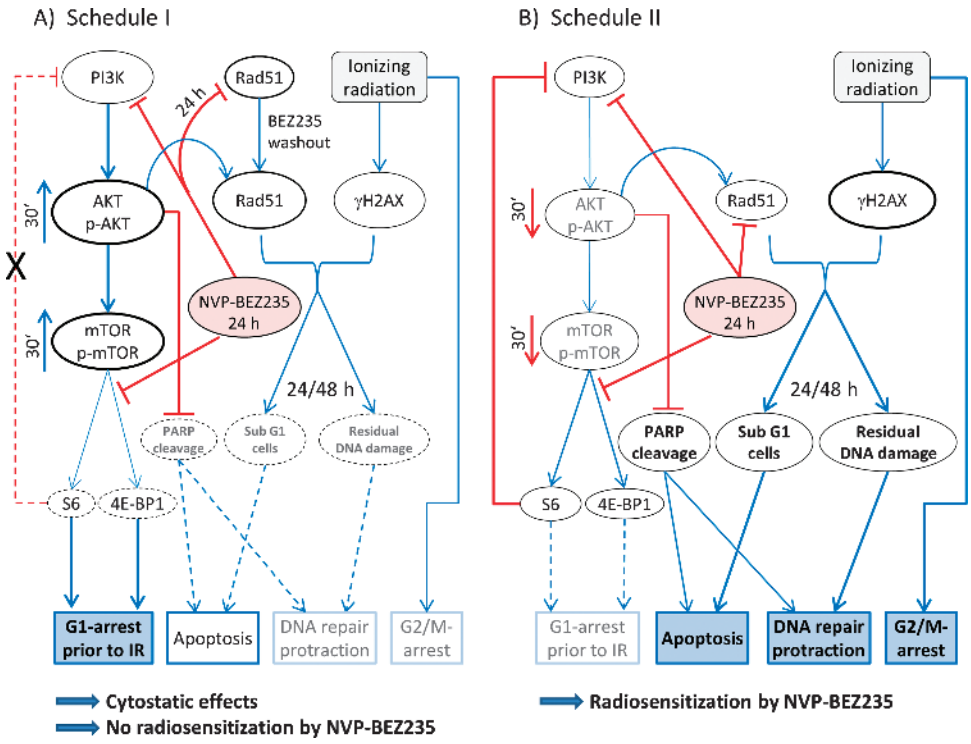

Figure 7. A simplified diagram of putative signaling pathways accountable for the differential responses of tumor cells to a dual PI3K/mTOR inhibition and ionizing radiation (IR) used in two different drug-irradiation schedules. Incubation of tumor cells with NVP-BEZ235 for 24 hours before IR (A) leads to an activation of the PI3K/AKT/mTOR pathway at the time of irradiation, most likely due to the inhibition of the negative feedback loop mediated by ribosomal protein S6 (Figures 3 and W2). Subsequently, the activated pro-survival kinase AKT prevents radiation-induced apoptosis. In contrast, under schedule II, AKT and mTOR are *suppressed* at the time of irradiation (B). Furthermore, incubation with NVP-BEZ235 for 24 hours causes an arrest in the G_1 phase (Figure 6 and Tables W2–W4). Due to the higher portion of G_1 phase cells, exposure to IR leads to a diminished induction of γH2AX in cells treated for 24 hours before IR, compared to controls and schedule II (Figures 5*A* and W6, *A–C*). Cells treated according schedule I show a reduced Rad51 level during IR. After drug removal, Rad51 returned to the normal level (Figure 5*B*), thus leading to full repair of DNA damage (Figures 5*A* and W6, *A–C*). In contrast, under schedule II the expression of Rad51 remained diminished 24 and 48 hours after IR (Figure 5*B*). This might have increased the fraction of cells with hypodiploid DNA content and protracted DNA damage repair (Figures 4, W5, and 6). Besides this, cells treated according to schedule II showed a strong G_2/M arrest after combined drug-IR treatment (Figure 6 and Table W4). To summarize, schedule I caused a cytostatic effect, whereas schedule II gave rise to a strong radiosensitization (take note of the size of the letters/symbols and the thickness of the lines).

the interruption of the negative feedback loops that downregulate PI3K signaling, which in turn can paradoxically promote cell survival, as reported in case of rapalogs elsewhere [43–45]. This mechanism would explain the lack of radiosensitization by NVP-BEZ235 used in schedule I (i.e., long-term pretreatment).

In contrast to schedule I, tumor cells exposed only briefly to NVP-BEZ235 under schedule II exhibited reduced expression of phospho-AKT and phospho-mTOR (Figure 7*B*) after irradiation and, to a lesser extent, without IR exposure. Consistent with this observation, simultaneous drug-IR treatment according to schedule II caused late-stage apoptosis in DK-MG, GaMG, and U373 cell lines as evidenced by the increased fractions of cells with hypodiploid DNA content and cellular debris (Figures 4 and W5). In agreement with our data, Fokas et al. have found that NVP-BEZ235 increased both apoptosis and necrosis in SQ20B cells, without inducing apoptosis in FaDu cells [31]. Several studies have shown *cell type–specific* induction of apoptosis by NVP-BEZ235. Thus, NVP-BEZ235 has induced apoptosis in lung carcinoma, sarcoma, and leukemia [29,46] but not in glioma cell lines [47,48].

A further critical determinant of radiation-induced cell death is the induction and repair of DNA double-strand breaks, probed in this study by the expression of histone γH2AX (Figures 5 and W6, *A*–*C*). We found that the kinetics of DNA damage repair differed markedly between two treatment protocols. In cell samples pretreated with the NVP-BEZ235 under schedule I, the DNA damage completely recovered 48 hours after IR. In contrast, cells treated according schedule II showed high residual DNA damage levels up to 48 hours after IR, probably because of the NVP-BEZ235–mediated impairment of the homologous recombination mechanism of DNA repair.

In addition to the above effects, long-term treatment with NVP-BEZ235 before IR (schedule I) caused a substantial G_1 arrest. As a result, irradiation of G_1-arrested cells under schedule I induced even less DNA damage, compared to exponentially growing culture (Figure 5). Combined drug-IR treatment under schedule II caused a strong G_2/M block compared to irradiation alone (Table W4).

In summary, our study corroborates the importance of the drug administration schedule for combined tumor treatment reported previously [42] and also provides the first evidence that prolonged treatment of tumor cells with the dual PI3K and mTOR inhibitor NVP-BEZ235 did not sensitize glioblastoma cell lines to ionizing radiation. A possible reason could be the drug-mediated activation of PI3K and mTOR proteins. Yet the observed strong arrest of tumor cells in the G_1 phase justified the use of the substance as a strong cytostatic drug, which is currently being tested in clinical trials (phases I to II; www.clinicaltrials.gov). Finally, our *in vitro* data reveal the importance of the sequence of drug and IR schedule for the radiosensitizing of tumor cells and pave the way for future exploration of combination of molecularly targeted therapy and radiation on mouse xenograft tumor models.

Acknowledgments

We thank Gerald Büchold for the construction of the irradiation device.

References

[1] Walker MD, Alexander E Jr, Hunt WE, MacCarty CS, Mahaley MS Jr, Mealey J Jr, Norrell HA, Owens G, Ransohoff J, Wilson CB, et al. (1978). Evaluation of BCNU and/or radiotherapy in the treatment of anaplastic gliomas. A cooperative clinical trial. *J Neurosurg* **49**, 333–343.

[2] Stupp R, Mason WP, van den Bent MJ, Weller M, Fisher B, Taphoorn MJ, Belanger K, Brandes AA, Marosi C, Bogdahn U, et al. (2005). Radiotherapy plus concomitant and adjuvant temozolomide for glioblastoma. *N Engl J Med* **352**, 987–996.

[3] Chang CH, Horton J, Schoenfeld D, Salazer O, Perez-Tamayo R, Kramer S, Weinstein A, Nelson JS, and Tsukada Y (1983). Comparison of postoperative radiotherapy and combined postoperative radiotherapy and chemotherapy in the multidisciplinary management of malignant gliomas. A joint Radiation Therapy Oncology Group and Eastern Cooperative Oncology Group study. *Cancer* **52**, 997–1007.

[4] Hofer S and Herrmann R (2001). Chemotherapy for malignant brain tumors of astrocytic and oligodendroglial lineage. *J Cancer Res Clin Oncol* **127**, 91–95.

[5] Fan Q-W and Weiss WA (2010). Targeting the RTK-PI3K-mTOR axis in malignant glioma: overcoming resistance. *Curr Top Microbiol Immunol* **347**, 279–296.

[6] El-Deiry WS (2003). The role of p53 in chemosensitivity and radiosensitivity. *Oncogene* **22**, 7486–7495.

[7] Nicholson KM and Anderson NG (2002). The protein kinase B/Akt signalling pathway in human malignancy. *Cell Signal* **14**, 381–395.

[8] Nakashio A, Fujita N, Rokudai S, Sato S, and Tsuruo T (2000). Prevention of phosphatidylinositol 3′-kinase-Akt survival signaling pathway during topotecan-induced apoptosis. *Cancer Res* **60**, 5303–5309.

[9] Janmaat ML, Kruyt FA, Rodriguez JA, and Giaccone G (2003). Response to epidermal growth factor receptor inhibitors in non-small cell lung cancer cells: limited antiproliferative effects and absence of apoptosis associated with persistent activity of extracellular signal-regulated kinase or Akt kinase pathways. *Clin Cancer Res* **9**, 2316–2326.

[10] Vivanco I and Sawyers CL (2002). The phosphatidylinositol 3-kinase AKT pathway in human cancer. *Nat Rev Cancer* **2**, 489–501.

[11] Bjornsti MA and Houghton PJ (2004). The TOR pathway: a target for cancer therapy. *Nat Rev Cancer* **4**, 335–348.

[12] Xia S, Zhao Y, Yu S, and Zhang M (2010). Activated PI3K/Akt/COX-2 pathway induces resistance to radiation in human cervical cancer HeLa cells. *Cancer Biother Radiopharm* **25**, 317–323.

[13] Rudner J, Ruiner CE, Handrick R, Eibl HJ, Belka C, and Jendrossek V (2010). The Akt-inhibitor Erufosine induces apoptotic cell death in prostate cancer cells and increases the short term effects of ionizing radiation. *Radiat Oncol* **5**, 108.

[14] Zhang T, Cui GB, Zhang J, Zhang F, Zhou YA, Jiang T, and Li XF (2010). Inhibition of PI3 kinases enhances the sensitivity of non-small cell lung cancer cells to ionizing radiation. *Oncol Rep* **24**, 1683–1689.

[15] Kao GD, Jiang Z, Fernandes AM, Gupta AK, and Maity A (2007). Inhibition of phosphatidylinositol-3-OH kinase/Akt signaling impairs DNA repair in glioblastoma cells following ionizing radiation. *J Biol Chem* **282**, 21206–21212.

[16] Li H-F, Kim J-S, and Waldman T (2009). Radiation-induced Akt activation modulates radioresistance in human glioblastoma cells. *Radiat Oncol* **4**, 43.

[17] Chen H, Ma Z, Vanderwaal RP, Feng Z, Gonzalez-Suarez I, Wang S, Zhang J, Roti Roti JL, Gonzalo S, and Zhang J (2011). The mTOR inhibitor rapamycin suppresses DNA double-strand break repair. *Radiat Res* **175**, 214–224.

[18] Gottschalk AR, Doan A, Nakamura JL, Stokoe D, and Haas-Kogan DA (2005). Inhibition of phosphatidylinositol-3-kinase causes increased sensitivity to radiation through a PKB-dependent mechanism. *Int J Radiat Oncol Biol Phys* **63**, 1221–1227.

[19] Manning BD (2004). Balancing Akt with S6K: implications for both metabolic diseases and tumorigenesis. *J Cell Biol* **167**, 399–403.

[20] Markman B, Dienstmann R, and Tabernero J (2010). Targeting the PI3K/Akt/mTOR pathway—beyond rapalogs. *Oncotarget* **1**, 530–543.

[21] Wan X, Harkavy B, Shen N, Grohar P, and Helman LJ (2006). Rapamycin induces feedback activation of Akt signaling through an IGF-1R-dependent mechanism. *Oncogene* **26**, 1932–1940.

[22] Stein RC (2001). Prospects for phosphoinositide 3-kinase inhibition as a cancer treatment. *Endocr Relat Cancer* **8**, 237–248.

[23] Gupta AK, Cerniglia GJ, Mick R, Ahmed MS, Bakanauskas VJ, Muschel RJ, and McKenna WG (2003). Radiation sensitization of human cancer cells *in vivo* by inhibiting the activity of PI3K using LY294002. *Int J Radiat Oncol Biol Phys* **56**, 846–853.

[24] Maira SM, Stauffer F, Brueggen J, Furet P, Schnell C, Fritsch C, Brachmann S, Chène P, De Pover A, Schoemaker K, et al. (2008). Identification and characterization of NVP-BEZ235, a new orally available dual phosphatidylinositol 3-kinase/mammalian target of rapamycin inhibitor with potent *in vivo* antitumor activity. *Mol Cancer Ther* **7**, 1851–1863.

[25] Blatt K, Herrmann H, Mirkina I, Hadzijusufovic E, Peter B, Strommer S, Hoermann G, Mayerhofer M, Hoetzenecker K, Klepetko W, et al. (2012). The PI3-kinase/mTOR-targeting drug NVP-BEZ235 inhibits growth and IgE-dependent activation of human mast cells and basophils. *PLoS One* **7**, e29925.

[26] Cho DC, Cohen MB, Panka DJ, Collins M, Ghebremichael M, Atkins MB, Signoretti S, and Mier JW (2010). The efficacy of the novel dual PI3-kinase/mTOR inhibitor NVP-BEZ235 compared with rapamycin in renal cell carcinoma. *Clin Cancer Res* **16**, 3628–3638.

[27] Kong D and Yamori T (2008). Phosphatidylinositol 3-kinase inhibitors: promising drug candidates for cancer therapy. *Cancer Sci* **99**, 1734–1740.

[28] Xu CX, Li Y, Yue P, Owonikoko TK, Ramalingam SS, Khuri FR, and Sun SY (2011). The combination of RAD001 and NVP-BEZ235 exerts synergistic anticancer activity against non-small cell lung cancer *in vitro* and *in vivo*. *PLoS One* **6**, e20899.

[29] Konstantinidou G, Bey EA, Rabellino A, Schuster K, Maira MS, Gazdar AF, Amici A, Boothman DA, and Scaglioni PP (2009). Dual phosphoinositide 3-kinase/mammalian target of rapamycin blockade is an effective radiosensitizing strategy for the treatment of non-small cell lung cancer harboring K-RAS mutations. *Cancer Res* **69**, 7644–7652.

[30] Fokas E, Im JH, Hill S, Yameen S, Stratford M, Beech J, Hackl W, Maira SM, Bernhard EJ, McKenna WG, et al. (2012). Dual inhibition of the PI3K/mTOR pathway increases tumor radiosensitivity by normalizing tumor vasculature. *Cancer Res* **72**, 239–248.

[31] Fokas E, Yoshimura M, Prevo R, Higgins G, Hackl W, Maira SM, Bernhard EJ, McKenna WG, and Muschel RJ (2012). NVP-BEZ235 and NVP-BGT226, dual phosphatidylinositol 3-kinase/mammalian target of rapamycin inhibitors, enhance tumor and endothelial cell radiosensitivity. *Radiat Oncol* **7**, 48.

[32] Mukherjee B, Tomimatsu N, Amancherla K, Camacho CV, Pichamoorthy N, and Burma S (2012). The dual PI3K/mTOR inhibitor NVP-BEZ235 is a potent inhibitor of ATM- and DNA-PKCs-mediated DNA damage responses. *Neoplasia* **14**, 34–43.

[33] Azad A, Jackson S, Cullinane C, Natoli A, Neilsen PM, Callen DF, Maira SM, Hackl W, McArthur GA, and Solomon B (2011). Inhibition of DNA-dependent protein kinase induces accelerated senescence in irradiated human cancer cells. *Mol Cancer Res* **9**, 1696–1707.

[34] Djuzenova C, Mühl B, Schakowski R, Oppitz U, and Flentje M (2004). Normal expression of DNA repair proteins, hMre11, Rad50 and Rad51 but protracted formation of Rad50 containing foci in X-irradiated skin fibroblasts from radiosensitive cancer patients. *Br J Cancer* **90**, 2356–2363.

[35] Muslimovic A, Ismail IH, Gao Y, and Hammarsten O (2008). An optimized method for measurement of gamma-H2AX in blood mononuclear and cultured cells. *Nat Protoc* **3**, 1187–1193.

[36] Djuzenova CS, Sukhorukov VL, Klöck G, Arnold WM, and Zimmermann U (1994). Effect of electric field pulses on the viability and on the membrane-bound immunoglobulins of LPS-activated murine B-lymphocytes: correlation with the cell cycle. *Cytometry* **15**, 35–45.

[37] Manara MC, Nicoletti G, Zambelli D, Ventura S, Guerzoni C, Landuzzi L, Lollini PL, Maira SM, García-Echeverría C, Mercuri M, et al. (2010). NVP-BEZ235 as a new therapeutic option for sarcomas. *Clin Cancer Res* **16**, 530–540.

[38] Fingar DC, Richardson CJ, Tee AR, Cheatham L, Tsou C, and Blenis J (2004). mTOR controls cell cycle progression through its cell growth effectors S6K1 and 4E-BP1/eukaryotic translation initiation factor 4E. *Mol Cell Biol* **24**, 200–216.

[39] Foster DA, Yellen P, Xu L, and Saqcena M (2010). Regulation of G1 cell cycle progression: distinguishing the restriction point from a nutrient-sensing cell growth checkpoint(s). *Genes Cancer* **1**, 1124–1131.

[40] Rogakou EP, Pilch DR, Orr AH, Ivanova VS, and Bonner WM (1998). DNA double-stranded breaks induce histone H2AX phosphorylation on serine 139. *J Biol Chem* **273**, 5858–5868.

[41] Nyati MK, Morgan MA, Feng FY, and Lawrence TS (2006). Integration of EGFR inhibitors with radiochemotherapy. *Nat Rev Cancer* **6**, 876–885.

[42] Chun PY, Feng FY, Scheurer AM, Davis MA, Lawrence TS, and Nyati MK (2006). Synergistic effects of gemcitabine and gefitinib in the treatment of head and neck carcinoma. *Cancer Res* **66**, 981–988.

[43] Gulati N, Karsy M, Albert L, Murali R, and Jhanwar-Uniyal M (2009). Involvement of mTORC1 and mTORC2 in regulation of glioblastoma multiforme growth and motility. *Int J Oncol* **35**, 731–740.

[44] Julien L-A, Carriere A, Moreau J, and Roux PP (2010). mTORC1-activated S6K1 phosphorylates Rictor on threonine 1135 and regulates mTORC2 signaling. *Mol Cell Biol* **30**, 908–921.

[45] Rodrik-Outmezguine VS, Chandarlapaty S, Pagano NC, Poulikakos PI, Scaltriti M, Moskatel E, Baselga J, Guichard S, and Rosen N (2011). mTOR kinase inhibition causes feedback-dependent biphasic regulation of AKT signaling. *Cancer Discov* **1**, 248–259.

[46] Chiarini F, Grimaldi C, Ricci F, Tazzari PL, Evangelisti C, Ognibene A, Battistelli M, Falcieri E, Melchionda F, Pession A, et al. (2010). Activity of the novel dual phosphatidylinositol 3-kinase/mammalian target of rapamycin inhibitor NVP-BEZ235 against T-cell acute lymphoblastic leukemia. *Cancer Res* **70**, 8097–8107.

[47] Liu TJ, Koul D, LaFortune T, Tiao N, Shen RJ, Maira SM, Garcia-Echevrria C, and Yung WK (2009). NVP-BEZ235, a novel dual phosphatidylinositol 3-kinase/mammalian target of rapamycin inhibitor, elicits multifaceted antitumor activities in human gliomas. *Mol Cancer Ther* **8**, 2204–2210.

[48] Marone R, Erhart D, Mertz AC, Bohnacker T, Schnell C, Cmiljanovic V, Stauffer F, Garcia-Echeverria C, Giese B, Maira SM, et al. (2009). Targeting melanoma with dual phosphoinositide 3-kinase/mammalian target of rapamycin inhibitors. *Mol Cancer Res* **7**, 601–613.

Supplementary Materials

Antibodies

The primary antibodies used were rabbit polyclonal anti-PTEN, rabbit polyclonal anti-PI3K p110, rabbit polyclonal anti-PI3K p85, mouse monoclonal anti–phospho-AKT (Ser^{473}), rabbit polyclonal anti-AKT, rabbit monoclonal anti–phospho-mTOR (Ser^{2448}), rabbit polyclonal anti-mTOR, rabbit polyclonal anti–phospho-S6 ($Ser^{240/244}$), mouse monoclonal anti-S6, mouse monoclonal anti–phospho-4E-BP1 (all from Cell Signaling Technology, Danvers, MA), mouse monoclonal anti–β-actin (Sigma, Deisenhofen, Germany), and mouse monoclonal anti–phospho-histone H2AX (Ser^{139}) fluorescein isothiocyanate conjugate (Millipore, Schwalbach, Germany). Secondary species-specific antibodies for Western blot were labeled with HRP (DAKO, Hamburg, Germany).

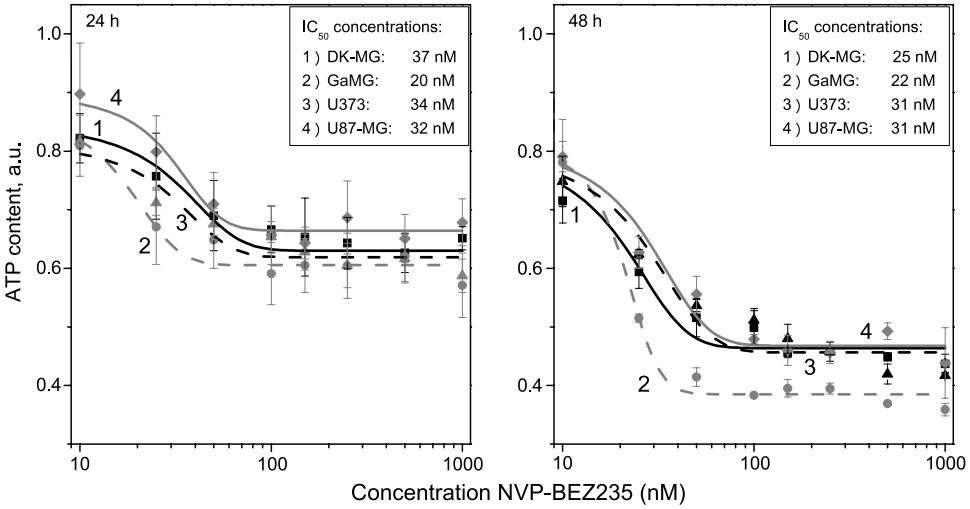

Figure W1. Changes of intracellular ATP in glioblastoma cells exposed to serial dilutions of NVP-BEZ235 for 24 and 48 hours. ATP content was measured by standard luciferase bioluminescence assay. Quadruplicate data derived from at least three independent experiments were averaged, normalized against non-treated controls (DMSO), and analyzed using the standard 4PLM (Equation 1) to generate dose-response curves. Error bars indicate SD values. Depicted are the calculated IC_{50} concentrations.

Table W1. PEs and Radiosensitivity Parameters of Control, Irradiated, and/or Drug-Treated Tumor Cell Lines under Two Different Drug-IR Schedules.

Cell Line	Treatment		PE*	SF2†		D_{10}‡		I_{10} ($D_{10\ Control}/D_{10\ NVP\text{-}BEZ235}$)
DK-MG	Schedule I	Control	0.22 ± 0.06	0.63 ± 0.12		5.73 ± 0.93		1.08 ± 0.18
		BEZ235	0.18 ± 0.04	0.58 ± 0.12		5.33 ± 0.73		
	Schedule II	Control	0.17 ± 0.09	0.67 ± 0.09	§	7.93 ± 0.54	§	1.92 ± 0.16
		BEZ235	0.16 ± 0.08	0.38 ± 0.05		4.15 ± 0.25		
U87-MG	Schedule I	Control	0.23 ± 0.15	0.54 ± 0.10		5.82 ± 0.35		0.89 ± 0.12
		BEZ235	0.18 ± 0.07	0.58 ± 0.04		6.46 ± 0.50		
	Schedule II	Control	0.20 ± 0.08	0.62 ± 0.02	§	8.52 ± 0.39	§	2.1 ± 0.14
		BEZ235	0.16 ± 0.09	0.36 ± 0.05		4.06 ± 0.31		
GaMG	Schedule I	Control	0.17 ± 0.04	0.74 ± 0.09		7.69 ± 0.80		1.00 ± 0.05
		BEZ235	0.14 ± 0.02	0.79 ± 0.04		7.69 ± 0.61		
	Schedule II	Control	0.17 ± 0.06	0.80 ± 0.08	§	10.21 ± 2.32	§	2.21 ± 0.48
		BEZ235	0.17 ± 0.06	0.46 ± 0.08		4.64 ± 0.51		
U373	Schedule I	Control	0.38 ± 0.18	0.64 ± 0.12		6.01 ± 0.50		0.99 ± 0.11
		BEZ235	0.35 ± 0.02	0.59 ± 0.02		6.15 ± 0.83		
	Schedule II	Control	0.29 ± 0.07	0.74 ± 0.08	§	9.01 ± 0.61	§	2.51 ± 0.58
		BEZ235	0.30 ± 0.07	0.30 ± 0.09		3.81 ± 1.14		

Data are presented as means (±SD) from at least four independent experiments. For detailed description, see legend to Figure 2.

*PE, plating efficiency.

†SF2, surviving fraction at 2 Gy.

‡D_{10}, radiation dose yielding 10% survival; I_{10}, growth inhibition factor was calculated as (D_{10} control)/D_{10} + inhibitor).

§$\triangleq$ < .05.

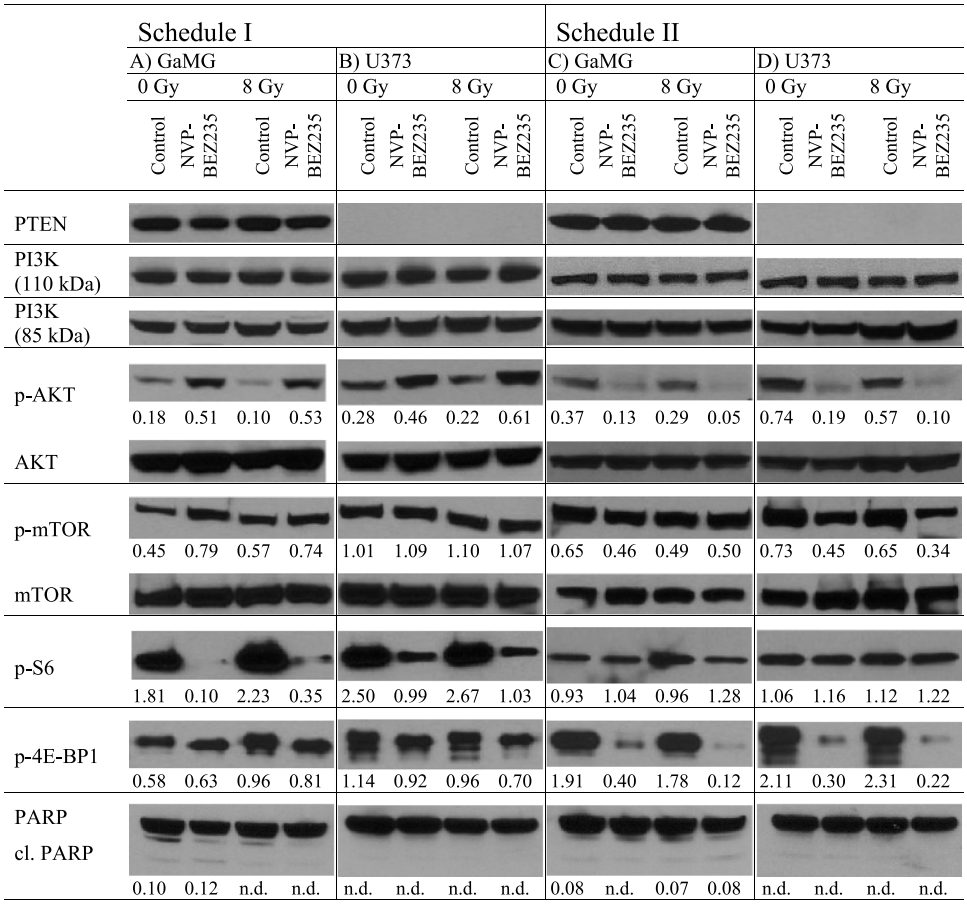

Figure W2. Effects of NVP-BEZ235 and IR on the expression levels of marker proteins in GaMG (A, C) and U373 (B, D) cell lines detected 30 minutes after IR. Cells were treated with NVP-BEZ235 and IR either in schedule I (left side) or schedule II (right side). For details, see legend to Figure 3. n.d. indicates not determined.

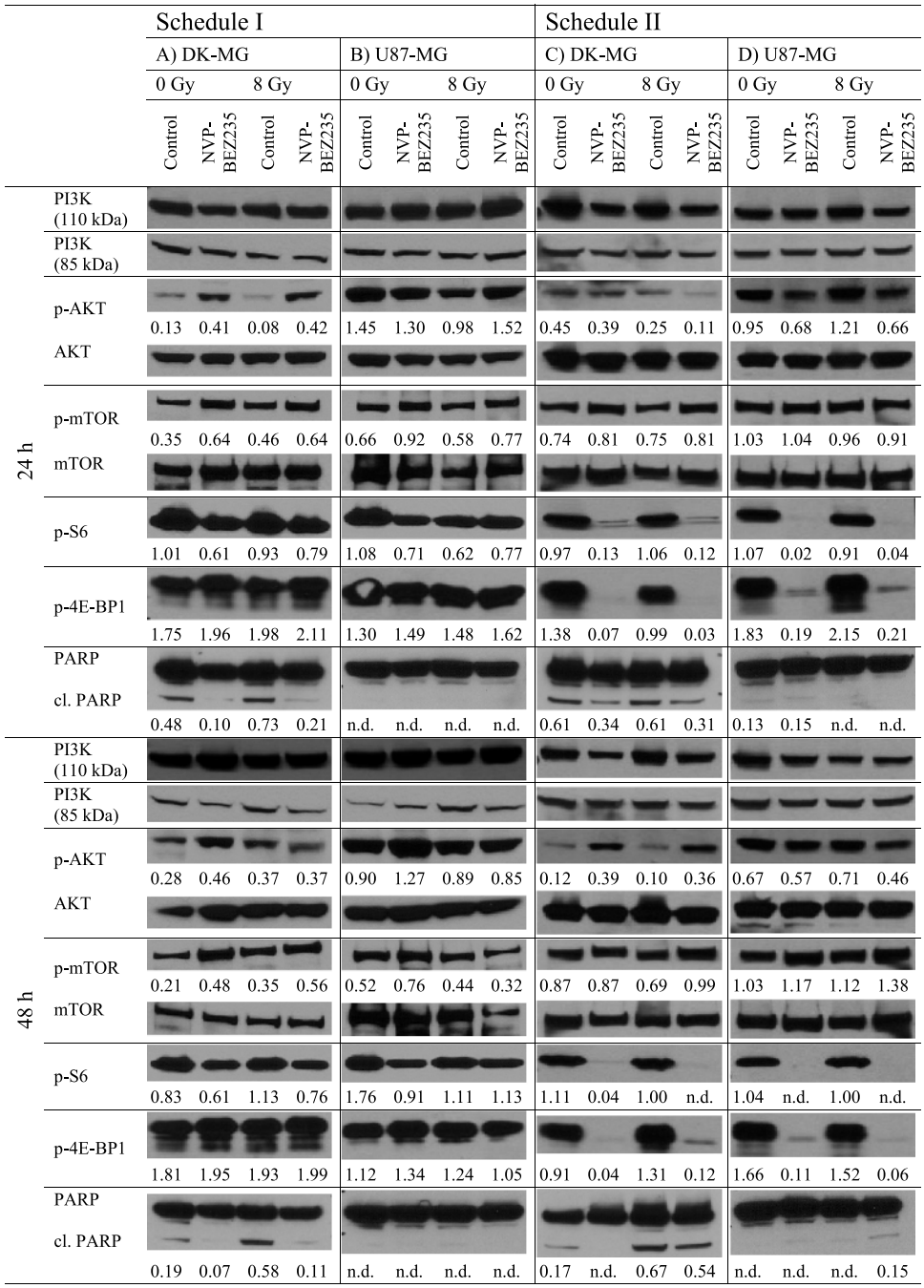

Figure W3. Effects of NVP-BEZ235 and IR on the expression levels of marker proteins in DK-MG (A, C) and U87-MG (B, D) cell lines detected 24 and 48 hours after IR. Cells were treated with NVP-BEZ235 and IR either in schedule I (left side) or schedule II (right side). For details, see legend to Figure 3.

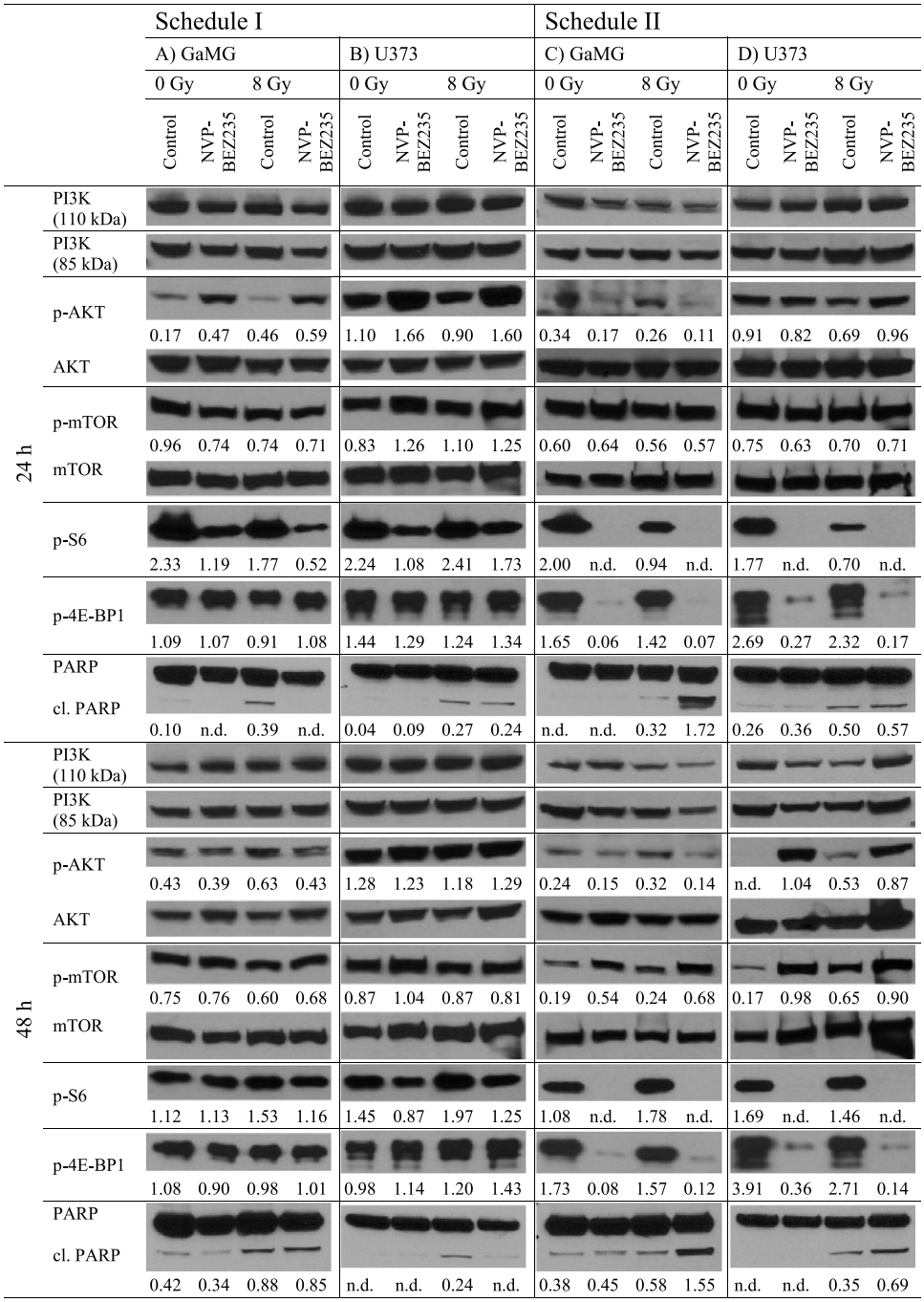

Figure W4. Effects of NVP-BEZ235 and IR on the expression levels of marker proteins in GaMG (A, C) and U373 (B, D) cell lines detected 24 and 48 hours after IR. Cells were treated with NVP-BEZ235 and IR either in schedule I (left side) or schedule II (right side). For details, see legend to Figure 3.

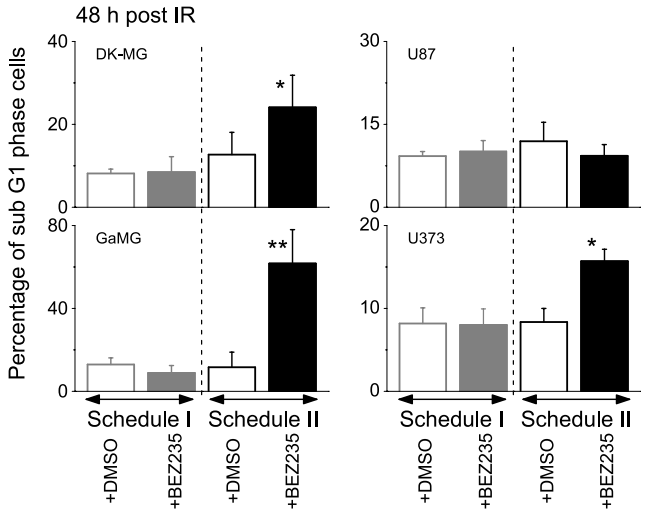

Figure W5. Effects of NVP-BEZ235 and IR on the late-stage apoptosis (subG$_1$ cells). Cells were treated with NVP-BEZ235 and IR either in schedule I or schedule II. For details, see legend to Figure 4.

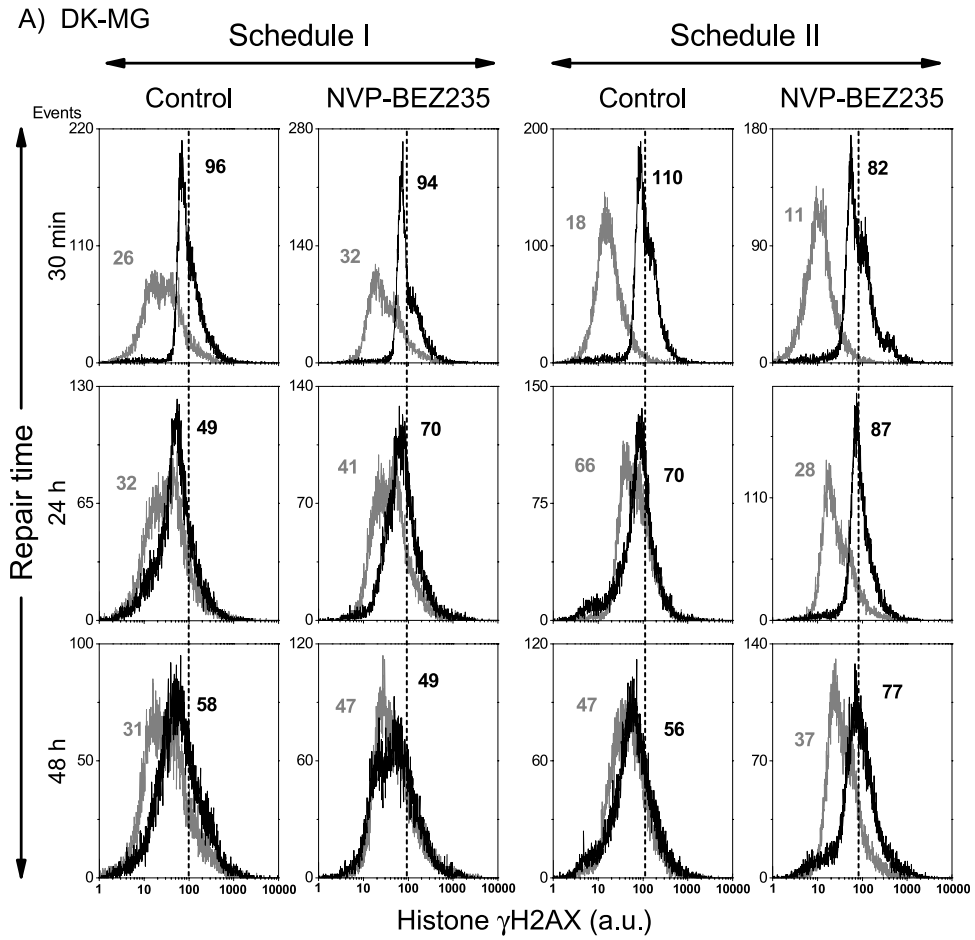

Figure W6. (A) Effects of NVP-BEZ235 and IR on the induction and repair of DNA damage in DK-MG (A) cell line. Cells were treated with NVP-BEZ235 and IR either in schedule I (left side) or schedule II (right side). For details, see legend to Figure 5. (B) Effects of NVP-BEZ235 and IR on the induction and repair of DNA damage in U87-MG cell line. Cells were treated with NVP-BEZ235 and IR either in schedule I (left side) or schedule II (right side). For details, see legend to Figure 5. (C) Effects of NVP-BEZ235 and IR on the induction and repair of DNA damage in U373 cell line. Cells were treated with NVP-BEZ235 and IR either in schedule I (left side) or schedule II (right side). For details, see legend to Figure 5.

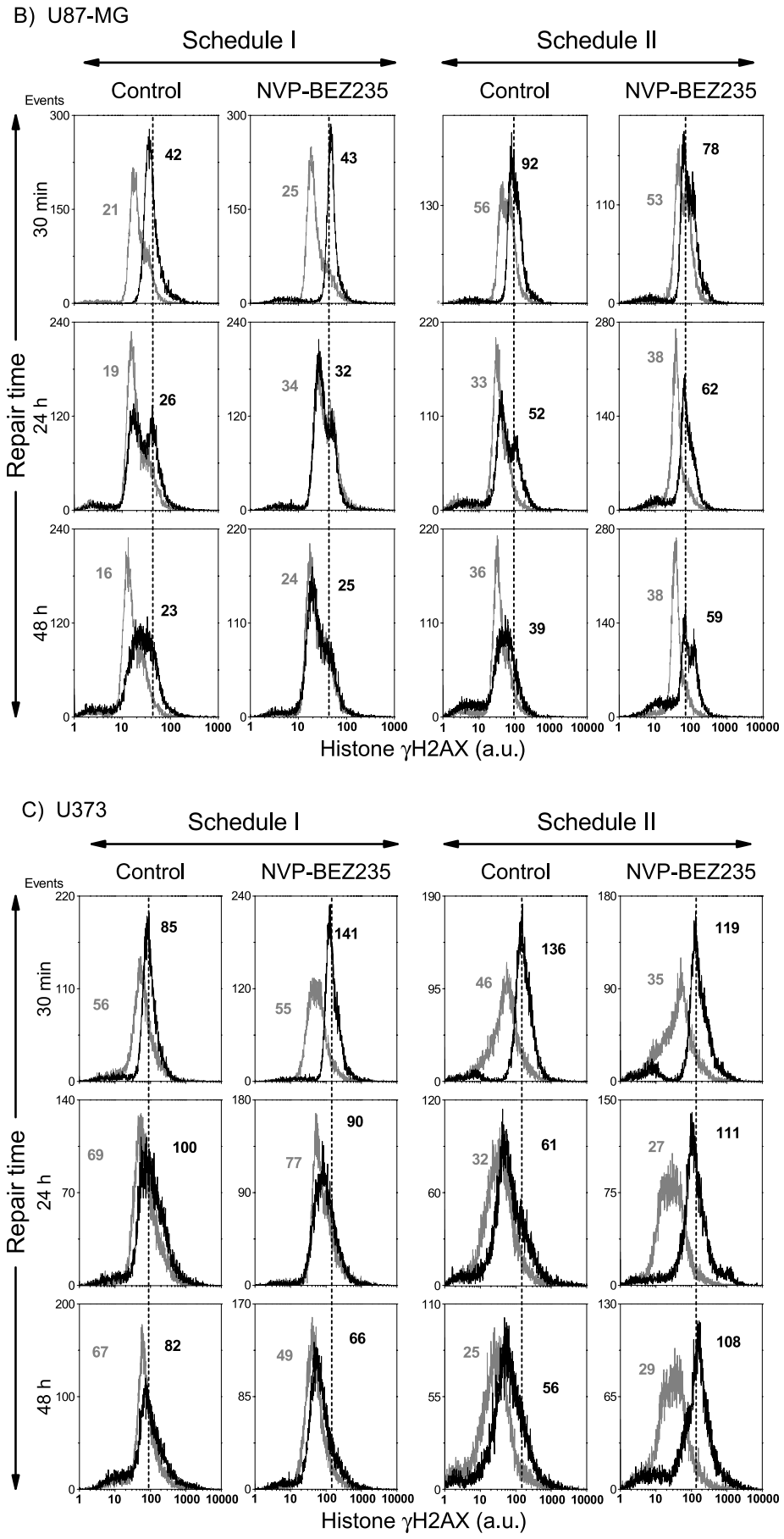

Figure W6. (*continued*).

Table W2. Cell Cycle Phase Distribution in Tumor Cells Treated with NVP-BEZ235 and IR according to Different Schedules.

Cell Line	Treatment Modality			G_0/G_1 (%)	S (%)	G_2/M (%)	G_2/G_1
DK-MG	Schedule I	0 Gy	Control	53 ± 4	22 ± 3	26 ± 3	0.49
			NVP-BEZ235	73 ± 2	9 ± 2	18 ± 2	0.25
		8 Gy	Control	54 ± 3	21 ± 3	25 ± 3	0.46
			NVP-BEZ235	74 ± 2	10 ± 2	17 ± 2	0.23
	Schedule II	0 Gy	Control	46 ± 4	28 ± 3	26 ± 3	0.57
			NVP-BEZ235	45 ± 4	29 ± 5	26 ± 3	0.58
		8 Gy	Control	46 ± 4	28 ± 3	26 ± 4	0.57
			NVP-BEZ235	46 ± 5	28 ± 3	26 ± 4	0.57
U87-MG	Schedule I	0 Gy	Control	70 ± 3	20 ± 3	10 ± 2	0.14
			NVP-BEZ235	90 ± 4	6 ± 2	5 ± 2	0.06
		8 Gy	Control	71 ± 3	19 ± 2	10 ± 4	0.14
			NVP-BEZ235	89 ± 3	6 ± 1	5 ± 2	0.06
	Schedule II	0 Gy	Control	51 ± 8	28 ± 3	22 ± 6	0.43
			NVP-BEZ235	51 ± 9	28 ± 3	21 ± 6	0.41
		8 Gy	Control	49 ± 9	29 ± 4	22 ± 7	0.45
			NVP-BEZ235	50 ± 9	28 ± 4	22 ± 6	0.44
GaMG	Schedule I	0 Gy	Control	60 ± 6	28 ± 4	12 ± 4	0.20
			NVP-BEZ235	80 ± 3	11 ± 4	9 ± 4	0.11
		8 Gy	Control	61 ± 7	27 ± 5	12 ± 5	0.20
			NVP-BEZ235	79 ± 3	13 ± 5	8 ± 3	0.10
	Schedule II	0 Gy	Control	40 ± 12	34 ± 11	26 ± 16	0.65
			NVP-BEZ235	41 ± 11	36 ± 11	23 ± 16	0.56
		8 Gy	Control	40 ± 12	35 ± 12	25 ± 16	0.63
			NVP-BEZ235	42 ± 11	33 ± 16	24 ± 18	0.57
U373	Schedule I	0 Gy	Control	67 ± 6	17 ± 3	16 ± 5	0.25
			NVP-BEZ235	65 ± 11	19 ± 7	16 ± 4	0.25
		8 Gy	Control	65 ± 5	18 ± 3	17 ± 5	0.26
			NVP-BEZ235	62 ± 10	21 ± 6	17 ± 5	0.27
	Schedule II	0 Gy	Control	36 ± 8	37 ± 13	28 ± 10	0.78
			NVP-BEZ235	38 ± 10	37 ± 13	25 ± 11	0.66
		8 Gy	Control	39 ± 9	36 ± 13	25 ± 9	0.64
			NVP-BEZ235	38 ± 10	37 ± 13	24 ± 11	0.63

Thirty minutes after IR, cells were fixed, permeabilized, stained with PI, and analyzed for DNA content by flow cytometry.
Data are presented as means (±SD) from at least four independent experiments. For detailed description, see legend to Figure 6.

Table W3. Cell Cycle Phase Distribution in Tumor Cells Treated with NVP-BEZ235 and IR according to Different Schedules.

Cell Line	Treatment Modality			G_0/G_1 (%)	S (%)	G_2/M (%)	G_2/G_1
DK-MG	Schedule I	0 Gy	Control	49 ± 3	24 ± 4	27 ± 3	0.55
			NVP-BEZ235	49 ± 9	26 ± 4	25 ± 6	0.51
		8 Gy	Control	21 ± 4	8 ± 1	71 ± 4	3.38
			NVP-BEZ235	22 ± 12	31 ± 4	47 ± 12	2.14
	Schedule II	0 Gy	Control	55 ± 6	22 ± 2	23 ± 6	0.42
			NVP-BEZ235	74 ± 6	9 ± 2	17 ± 6	0.23
		8 Gy	Control	29 ± 13	9 ± 3	63 ± 16	2.17
			NVP-BEZ235	27 ± 16	11 ± 3	62 ± 13	2.30
U87-MG	Schedule I	0 Gy	Control	71 ± 3	18 ± 2	10 ± 1	0.14
			NVP-BEZ235	67 ± 3	20 ± 4	14 ± 2	0.21
		8 Gy	Control	58 ± 6	10 ± 1	32 ± 5	0.55
			NVP-BEZ235	56 ± 8	19 ± 4	25 ± 6	0.45
	Schedule II	0 Gy	Control	68 ± 8	20 ± 2	12 ± 6	0.18
			NVP-BEZ235	85 ± 7	9 ± 2	6 ± 6	0.07
		8 Gy	Control	59 ± 14	9 ± 1	33 ± 15	0.56
			NVP-BEZ235	58 ± 17	4 ± 3	37 ± 15	0.64
GaMG	Schedule I	0 Gy	Control	73 ± 7	18 ± 5	9 ± 3	0.12
			NVP-BEZ235	50 ± 14	26 ± 5	24 ± 4	0.48
		8 Gy	Control	65 ± 6	17 ± 4	17 ± 4	0.26
			NVP-BEZ235	27 ± 9	22 ± 5	51 ± 9	1.89
	Schedule II	0 Gy	Control	62 ± 4	28 ± 3	11 ± 3	0.18
			NVP-BEZ235	79 ± 6	12 ± 5	9 ± 2	0.11
		8 Gy	Control	55 ± 12	26 ± 4	19 ± 6	0.35
			NVP-BEZ235	40 ± 8	12 ± 4	47 ± 8	1.18
U373	Schedule I	0 Gy	Control	67 ± 7	12 ± 2	21 ± 5	0.31
			NVP-BEZ235	62 ± 5	15 ± 2	23 ± 3	0.37
		8 Gy	Control	57 ± 8	8 ± 3	35 ± 6	0.61
			NVP-BEZ235	37 ± 8	14 ± 3	49 ± 8	1.32
	Schedule II	0 Gy	Control	64 ± 5	18 ± 4	19 ± 3	0.30
			NVP-BEZ235	59 ± 5	24 ± 3	17 ± 2	0.29
		8 Gy	Control	60 ± 5	10 ± 2	30 ± 6	0.50
			NVP-BEZ235	24 ± 27	12 ± 5	64 ± 27	2.67

Twenty-four hours after IR, cells were fixed, permeabilized, stained with PI, and analyzed for DNA content by flow cytometry.
Data are presented as means (±SD) from at least four independent experiments. For detailed description, see legend to Figure 6.

Table W4. Cell Cycle Phase Distribution in Tumor Cells Treated with NVP-BEZ235 and IR according to Different Schedules.

Cell Line	Treatment Modality			G_0/G_1 (%)	S (%)	G_2/M (%)	G_2/G_1
DK-MG	Schedule I	0 Gy	Control	56 ± 4	20 ± 2	24 ± 3	0.43
			NVP-BEZ235	66 ± 7	13 ± 5	20 ± 4	0.30
		8 Gy	Control	39 ± 4	24 ± 2	37 ± 3	0.95
			NVP-BEZ235	53 ± 6	7 ± 3	41 ± 6	0.77
	Schedule II	0 Gy	Control	53 ± 4	23 ± 7	24 ± 6	0.45
			NVP-BEZ235	72 ± 3	10 ± 4	18 ± 2	0.25
		8 Gy	Control	37 ± 3	23 ± 3	40 ± 3	1.08
			NVP-BEZ235	26 ± 9	10 ± 6	64 ± 8	2.46
U87-MG	Schedule I	0 Gy	Control	71 ± 3	19 ± 2	10 ± 2	0.14
			NVP-BEZ235	70 ± 3	19 ± 2	11 ± 3	0.16
		8 Gy	Control	59 ± 2	17 ± 2	24 ± 2	0.41
			NVP-BEZ235	68 ± 3	14 ± 3	18 ± 3	0.26
	Schedule II	0 Gy	Control	69 ± 3	21 ± 3	11 ± 2	0.16
			NVP-BEZ235	82 ± 2	12 ± 1	6 ± 2	0.07
		8 Gy	Control	54 ± 2	20 ± 2	27 ± 2	0.50
			NVP-BEZ235	55 ± 2	8 ± 2	37 ± 1	0.67
GaMG	Schedule I	0 Gy	Control	87 ± 4	5 ± 3	8 ± 2	0.09
			NVP-BEZ235	81 ± 4	10 ± 3	10 ± 2	0.12
		8 Gy	Control	66 ± 8	12 ± 6	22 ± 4	0.33
			NVP-BEZ235	65 ± 4	18 ± 4	17 ± 3	0.26
	Schedule II	0 Gy	Control	77 ± 8	12 ± 5	11 ± 3	0.14
			NVP-BEZ235	80 ± 5	10 ± 3	10 ± 3	0.13
		8 Gy	Control	55 ± 6	21 ± 6	25 ± 6	0.45
			NVP-BEZ235	40 ± 7	11 ± 4	49 ± 9	1.23
U373	Schedule I	0 Gy	Control	82 ± 4	8 ± 2	10 ± 3	0.12
			NVP-BEZ235	79 ± 4	9 ± 2	12 ± 2	0.15
		8 Gy	Control	62 ± 8	16 ± 4	22 ± 5	0.35
			NVP-BEZ235	64 ± 5	15 ± 4	21 ± 3	0.33
	Schedule II	0 Gy	Control	70 ± 3	14 ± 2	16 ± 2	0.23
			NVP-BEZ235	68 ± 2	16 ± 2	16 ± 1	0.24
		8 Gy	Control	38 ± 5	22 ± 3	40 ± 4	1.05
			NVP-BEZ235	12 ± 5	14 ± 2	74 ± 6	6.17

Forty-eight hours after IR, cells were fixed, permeabilized, stained with PI, and analyzed for DNA content by flow cytometry.
Data are presented as means (±SD) from at least four independent experiments. For detailed description, see legend to Figure 6.